PHYSICAL REVIEW E **93**, 012704 (2016)

Phases and structures of sunset yellow and disodium cromoglycate mixtures in water

Akihiro Yamaguchi,[1] Gregory P. Smith,[1] Youngwoo Yi,[1] Charles Xu,[2,*] Silvia Biffi,[3] Francesca Serra,[3] Tommaso Bellini,[3] Chenhui Zhu,[4] and Noel A. Clark[1,†]

[1]*Soft Materials Research Center, University of Colorado, Boulder, Colorado 80309, USA*

[2]*Fairview High School, Boulder, Colorado 80305, USA*

[3]*Dipartimento di Biotecnologie Mediche e Medicina Traslazionale, Università degli Studi di Milano, Italy*

[4]*Advanced Light Source, Lawrence Berkeley National Laboratory, Berkeley, California 94720, USA*

(Received 14 November 2015; revised manuscript received 17 December 2015; published 12 January 2016)

We study phases and structures of mixtures of two representative chromonic liquid crystal materials, sunset yellow FCF (SSY) and disodium cromoglycate (DSCG), in water. A variety of combinations of isotropic, nematic (*N*), and columnar (also called *M*) phases are observed depending on their concentrations, and a phase diagram is made. We find a tendency for DSCG-rich regions to show higher-order phases while SSY-rich regions show lower-order ones. We observe uniform mesophases only when one of the materials is sparse in the *N* phases. Their miscibility in *M* phases is so low that essentially complete phase separation occurs. X-ray scattering and spectroscopy studies confirm that SSY and DSCG molecules do not mix when they form chromonic aggregates and neither do their aggregates when they form *M* phases.

DOI: 10.1103/PhysRevE.93.012704

I. INTRODUCTION

Understanding the formation of aggregates in mixtures of water-soluble materials and their organization is of interest in biophysics and materials science and engineering. Lyotropic chromonic liquid crystals (LCLCs) are anisotropic fluids formed when molecules with ionic peripherals and aromatic cores, found in food colorings and pharmaceuticals, are dissolved in water [1]. Because of their ionic groups, e.g., sulfonate or carboxylic groups, the molecules are soluble in water. On the other hand, they tend to stack on top of each other in water because of the hydrophobicity of the aromatic cores. Consequently, the molecules in the solution form polydispersed rodlike aggregates long enough to align relative to each other, similar to the formation of liquid crystal phases of very short double-helix deoxyribonucleic acids [2]. The solutions typically show isotropic (*I*), nematic (*N*), and columnar (*M*) phases, and coexistence of the phases depending on the concentration. LCLCs have been applied in optical components, organic electronics, bioengineering, and electrochemistry [3–7].

The most well-known LCLC materials are disodium cromoglycate (DSCG), also called cromolyn sodium, and sunset yellow FCF (SSY), also known as orange yellow S, as shown in Fig. 1. The hydrazone form of SSY is shown in the figure since it is more stable than the azo form in water [8]. The structures and phases of each are extensively studied. At high enough concentrations their solutions become nematic and columnar fluids [1]. The SSY molecule has a completely planar structure while DSCG has a slightly bent one; the sizes of SSY and DSCG along their long axes are 1.2 and 1.9 nm, respectively [9,10]. SSY has strong absorption in the blue and green region with an absorption peak near 480 nm while DSCG is transparent in the visible spectrum range. Both materials make linear aggregates in water by stacking their molecules on top of each other with stacking distances of about 3.4 Å [11,12].

Mixing the two chromonics raises various questions about the phases of the mixtures, the structures of the aggregates, and components of the aggregates. We study the phase behaviour of the LCLCs of ternary mixtures of SSY, DSCG, and water using polarized light microscopy, microspectroscopy, centrifugation, and x-ray diffraction. We present a ternary phase diagram of the mixtures and describe the miscibility and separation of the materials in various phases and in the chromonic aggregates.

II. EXPERIMENTS

(a) Preparation of the mixtures. SSY and DSCG were purchased from Sigma Aldrich. The purity of SSY was 90% and that of DSCG was 95% or above. The materials were weighed using a balance, and were put in 1.8 mL Eppendorf tubes, and then deionized water was added using a micropipet to achieve a target weight concentration denoted by (c_S,c_D), where c_S and c_D represent the weight percent (wt %) concentration of SSY and DSCG, respectively. Typical mixtures were heated in an oven kept at ∼60 °C for about 10 min to mix them evenly. Some of the mixtures with high concentration needed to be heated for a longer time at a higher temperature.

(b) Preparation of cells. A small amount of the mixture was dropped on a glass plate and then covered with another glass plate and then the mixture was sealed with mineral oil. As needed, one more glass plate was placed on the top plate of a cell to seal the material more thoroughly. To get a film with a known gap, an empty cell was fabricated by gluing the glass plates with epoxy mixed with spacers, then filled with a mixture by capillary force, and then sealed with mineral oil.

(c) Microscopy and spectroscopy. The mixtures were observed with a microscope with a polarizer and an analyzer. Depolarized transmission light microscopy (DTLM), in which the polarizer and analyzer are perpendicular to each other, was used to observe phases of the mixtures. Dichroism of the SSY of the cell was observed by removing either the polarizer or the analyzer. Both the polarizer and the analyzer

*Present address: Institute for Quantum Information and Matter, Caltech, Pasadena, CA 91125, USA.

†Corresponding author: noel.clark@colorado.edu

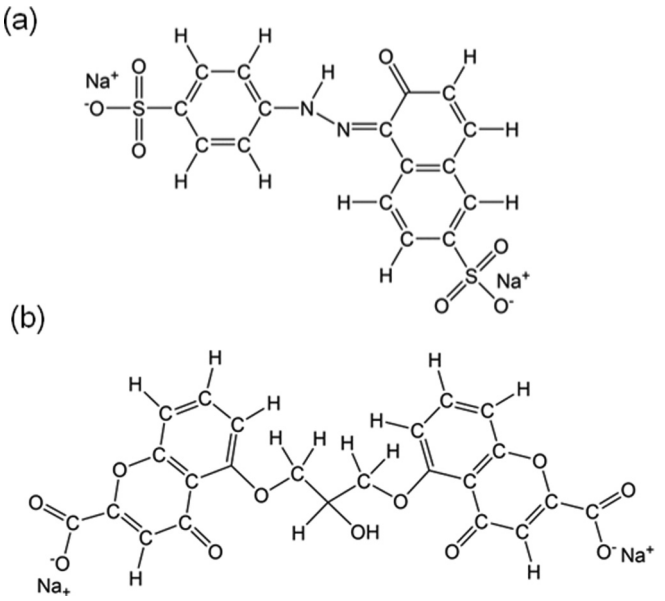

FIG. 1. Molecular structures of (a) hydrazone form of sunset yellow FCF (SSY) and (b) disodium cromoglycate (DSCG).

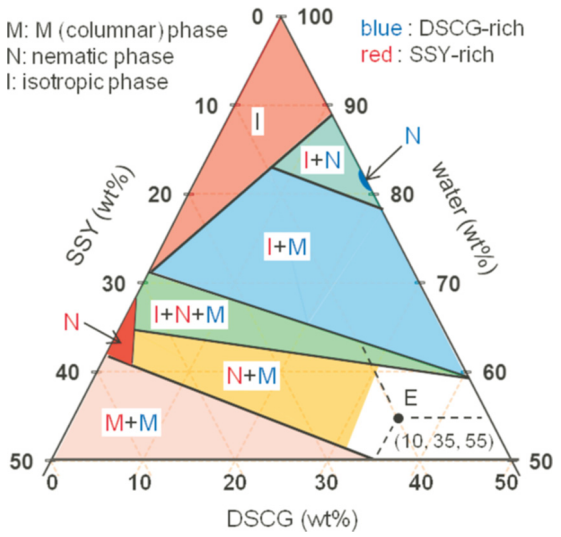

FIG. 2. Ternary phase diagram of mixtures of SSY and DSCG at room temperature. Various mixed phases are observed as well as pure *I*, *N* and *M* phases. Uniform *N* phases are found in very limited regions indicated with the arrows. Blue (dark gray) and red (light gray) colored letters represent DSCG-rich phases and SSY-rich phases, respectively. The point *E* is an example for the reading of the diagram, which indicates that the mixture is 10 wt % SSY, 35 wt % DSCG, and 55 wt % water.

were removed to detect the presence of SSY. Light from a small area on the image plane of the microscope was collected using an optical fiber and its spectrum was recorded using a spectrometer connected to the fiber to analyze the local c_S of the cells filled with the mixtures with a resolution of 10 μm.

(d) Centrifugation. Centrifugation was used to separate different phases of the mixtures in a capillary tube. Following centrifugation, the capillary was bisected at the observed interface between supernatant and pellet to separate the two fractions, and the absorbance of a diluted solution of each part was measured using a UV-VIS spectrometer to obtain c_S and c_D.

(e) X-ray scattering. The Advanced Light Source beamline 7.3.3 at Lawrence Berkeley National Lab was used to make x-ray diffraction measurements of the pure and mixed solutions of SSY and DSCG in capillaries with inner diameter of about 1 mm. Two-dimensional diffraction images were obtained using a Pilatus 2M detector, positioned at 32-cm away from the sample (wide angle x-ray scattering). The 2D images were reduced using NIKA software. Lorentzian fits were obtained to get both stacking or intermolecular distances in chromonic stacks and intercolumnar distances in *M* phases.

III. RESULTS AND ANALYSIS

A. Microscopy of the mixtures

The mixtures show various phases including *I*, *N*, and biphasic and triphasic coexistence of $I + N$, $I + N + M$, $I + M$, $N + M$, and $M + M$, as shown in Fig. 2. As expected, we find the *I* phase when both c_S and c_D are low. SSY and DSCG are uniformly mixed in this phase. When they are observed without the polarizer, the colors of the cells are uniform yellow, orange, or red depending on c_S and cell thickness. The two extreme ends of this phase meet with the phase transition concentration of each material.

Biphasic $I + N$ phases are observed near the two ends of the *I* region in the phase diagram [see Fig. 3(a)]. The domains in the *N* phase have relatively higher c_D than the domains in the *I* phase in both SSY-rich and DSCG-rich cases as can be seen from the colors of the images without the polarizer [see Fig. 3(b)].

Uniform *N* phases are found only when the concentration of one of the materials is small. For example, a uniform *N* phase is observed for the (0.5, 18) mixture while the (1, 18) mixture with an initial apparently uniform *N* phase produces small *I* domains after a thermal cycle. Figures 3(c) and 3(d) are DTLM images of the mixtures which show DSCG-dominant schlieren textures. Uniform *N* phases are also observed when c_D is low. The mixtures (35, 0.5), (33, 1), (35, 2), and (35, 3) have uniform *N* phases. For example, the microscope images of the mixture (33, 3) are shown in Figs. 3(e) and 3(f).

We often found the biphasic $I + M$ phase, coexistence of the SSY-rich *I* phase and the DSCG-rich *M* phase, as shown in Figs. 3(g) and 3(h). The M domains strongly expel SSY to form a columnar phase.

When c_S is larger than 1 wt %, the DSCG-dominant uniform *N* phase becomes the biphasic $I + N$ phase, as shown in Fig. 3(a). In this case, c_S values in the *I* domains are larger than those in the *N* domains. On the other hand, if c_D is larger than ~3 wt %, the SSY-dominant uniform *N* phase turns into the triphasic $I + N + M$ state or biphasic $N + M$ phase, as shown in Figs. 4(a) and 4(c). In this case, c_S of a lower-order domain is higher than that in a higher-order domain, as can be observed in Figs. 4(b) and 4(d). Biphasic $M + M$ phases are found when cells with low concentrations are dried gradually. Clear separation between the SSY-rich *M* phase and the DSCG-rich *M* phase is observed, as shown in Figs. 4(e) and 4(f) and Fig. 5.

Spinodal decomposition, the appearance of *M* domains in an *I*-phase background at high temperature which then

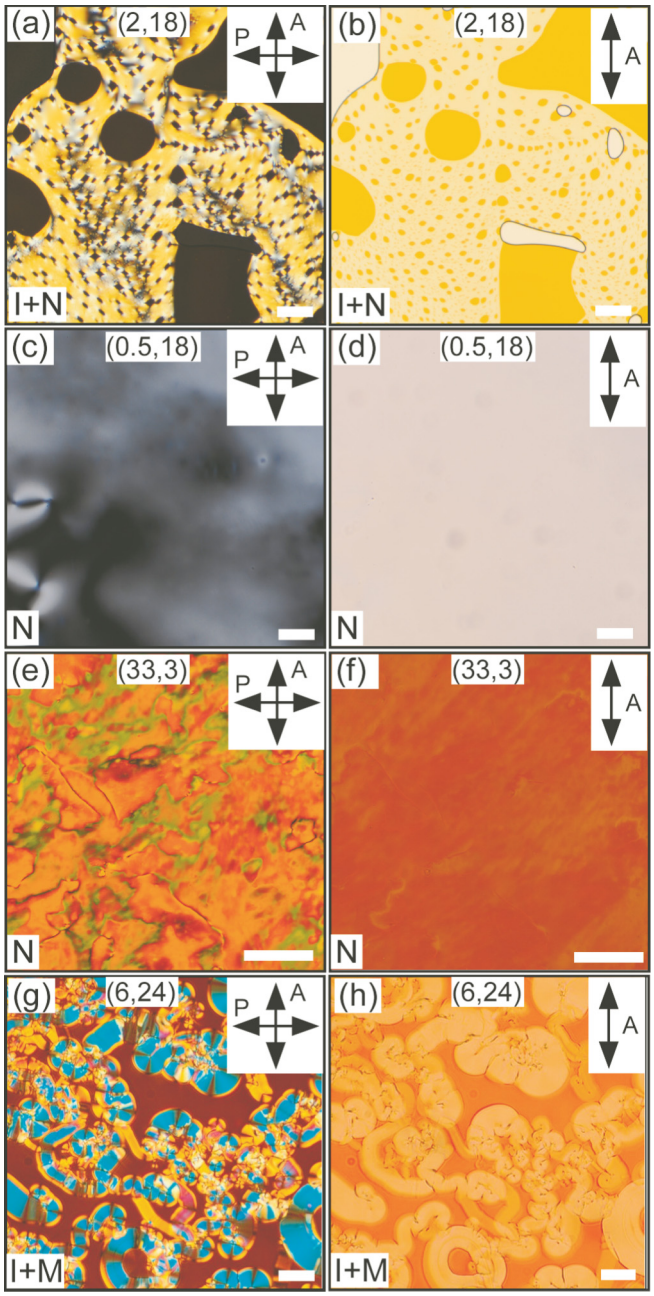

FIG. 3. Optical microscope images showing various phases. (a),(b) Coexistence of *I* and *N* phases in a cell with a mixture (2, 18), (c),(d) DSCG-dominant *N* phase of a cell with a mixture (0.5, 18), (e),(f) SSY-dominant *N* phase of a cell with a mixture (33, 3), and (g),(h) coexistence of *I* and *M* phases of a cell with a mixture (6, 24). Images on the left are taken with a polarizer and an analyzer perpendicular to each other and images on the right are taken with only an analyzer. Notice that there is no SSY dichroism in the image (d) while there is dichroism in the image (f). Also notice that the columnar DSCG domains in the image (h) have uniform light orange (light gray) color, indicating that a small amount of SSY is in the domain. The scale bars represent 100 μm.

turn into the *N* phase at lower temperature, is reported by Agra-Kooijman and co-workers in DSCG solution [13]. We observe a similar phenomenon in the mixture (2, 18) using optical microscopy, as shown in Fig. 6.

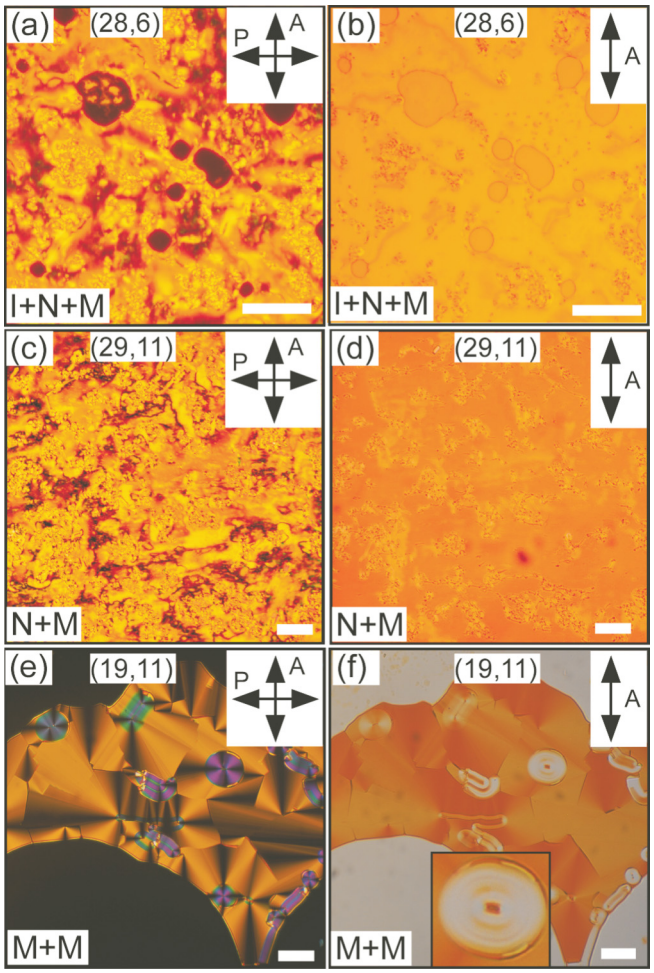

FIG. 4. Optical microscope images showing various other phases. (a),(b) Coexistence of *I*, *N*, and *M* phases in a thin cell with a mixture (28, 6), (c),(d) coexistence of *N* and *M* phases in a cell filled with a mixture (29, 11), and (e),(f) coexistence of SSY-dominant *M* phase and DSCG-dominant *M* phase of a cell filled with a mixture (19, 11) and dried for 16 days at room temperature. Images on the left are taken with a polarizer and an analyzer perpendicular to each other and image on the right are taken with only a polarizer. The inset in (f) shows separation of SSY in the DSCG-rich *M* phase. The scale bars represent 100 μm.

B. Microspectroscopy of DSCG-rich $I + N$ phase.

A cell filled with a mixture (2, 18) shows both *I* domains and *N* domains and c_S values of the domains change as the cell ages or undergoes thermal treatment, probably due to expelling of SSY aggregates from the *N* domains. The spectra in Fig. 7 show the progress of the separation of *I* and *N* phases by time and by a thermal cycle. After a week, c_S values of the *I* domains increase while those of *N* domains decrease. After a thermal cycle, during which the cell is heated up to 70 °C, above the clearing temperature of the cell, and then cooled down to room temperature, the coverage and the values of c_S of *I* domains increase while those of *N* domains decrease. Furthermore, the values of c_S of the same kind of domain are essentially indistinguishable after the thermal cycle.

The maximum values of the absorbance in *I* and *N* domains are 1.18 and 0.13, respectively. Using these values and the

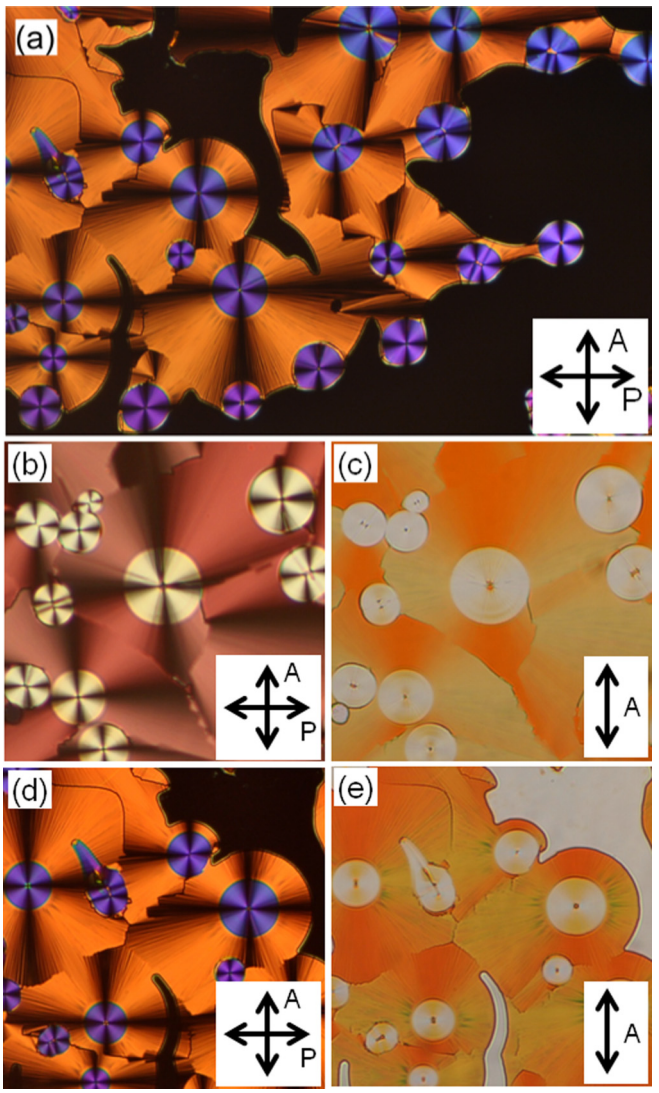

FIG. 5. Phase separation by gradual evaporation of water from a ternary mixture of SSY, DSCG, and water. Clear separations between SSY and DSCG can be seen from the DTLM images shown in (a), (b), and (d). The linear dichroism can also be seen under only an analyzer and the SSY aggregates on or in the DSCG domains also exhibit dichroism in (c) and (e). Notice that the DSCG domains that evolved earlier than SSY domains acted as a template for the orientation of the affected SSY aggregates. The black areas in (a) and (d) are filled with the mineral oil.

cell thickness, 12 μm, and the extinction coefficient of SSY, we find that the concentrations of I and N domains are roughly 2.6 wt % and 0.25 wt %, respectively. We use in the calculation of the concentrations the extinction coefficient of 20 000 $M^{-1}\,cm^{-1}$, which corresponds to the extinction coefficient at 0.09 wt % for I domains and 17 000 $M^{-1}\,cm^{-1}$ for N domains, which corresponds to 0.09 wt % according to Horowitz *et al.*, who report that the extinction coefficient of SSY varies from 23 000 to 17 000 $M^{-1}\,cm^{-1}$ as concentration varies from 0.002 wt % to 0.09 wt % [14]. Even though the concentrations of N domains are significantly larger than 0.09 wt %, the error will be minor since the trend in the reference shows that the decrease of the extinction coefficient slows down as the concentration increases.

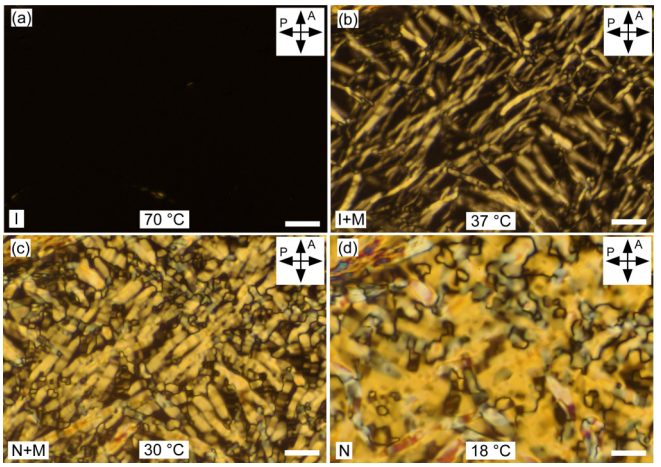

FIG. 6. Spinodal decomposition of a mixture (2, 18) observed by depolarized transmission light microscopy. (a),(b) As temperature decreases starting from the temperature showing the I phase, M phase nuclei appear and grow. (c),(d) As the coverage increases, M domains turn into N phase to cover the whole area. The scale bars represent 25 μm.

We also find that the spectrum measured after a week is broader than the spectrum of the fresh solution as shown in Figs. 7(b) and 7(a), respectively, which indicates that a progress of the aggregation of SSY molecules occurs by time. On the other hand, the spectrum becomes slightly narrower after the thermal cycling than that of the cell aged a week, as shown in Figs. 7(b) and 7(c), which suggests that the thermal cycle lowers the degree of the aggregation. We assume that the loss of water is negligible since the cell is double sealed with mineral oil and we observe increase of the coverage of I domains as time goes on and after the thermal cycling, which is not likely to happen if significant loss of water occurs in the cell.

A similar thermal cycle of a cell filled with a mixture (1, 18) changes the texture of the cell from an apparently uniform N phase into biphasic $I + N$. Interestingly, the absorbance of SSY in DSCG-rich N domains is independent of the orientation of the polarizer, which suggests that SSY is present in isotropic arrangement in the domains. There is a limited amount of SSY that can mix in the uniform DSCG-dominant N phase, which is $\sim$2% of the c_D. These results suggest that SSY molecules are not in DSCG aggregates but exist in random orientation in the phase. Short aggregates of SSY may coexist with the DSCG aggregates in the phase, or SSY molecules are bound on the surface of DSCG aggregates. The latter case is less likely to happen than the other because c_S further decreases to become negligible in the DSCG M phase, as shown in Fig. 7(c).

Spectroscopy study of supernatant and pellet fractions of capillary tubes of mixtures also reveals that supernatants have relatively more SSY and show lower-order phases while pellets have relatively more DSCG and show higher-order phases. For example, the supernatant fraction (I phase) of a mixture (2.3, 12.7) has about 30% higher c_S than that of the pellet fraction (N phase) and the supernatant fraction (N phase) of a mixture (10, 10) has 240% higher c_S than that of the pellet fraction (M phase). On the other hand, the pellets with the N and M phases have larger c_D than the supernatants by 40% and

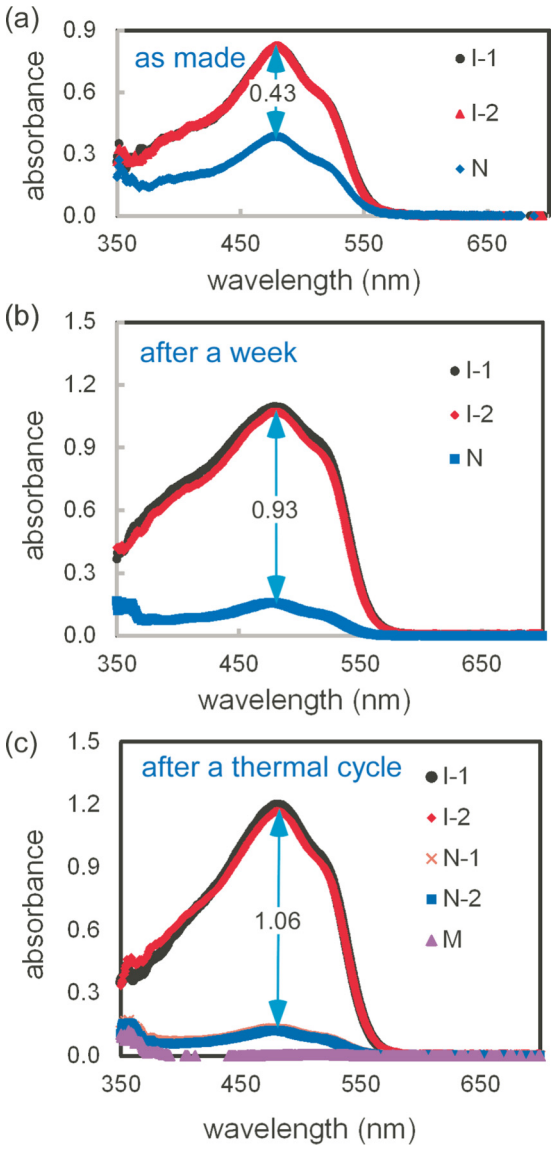

FIG. 7. Evolution of absorbance spectra of *I* and *N* domains of a thin cell (12 μm) with a mixture (2, 18). (a) Initial absorbance of two *I* domains, upper two lines made of (black) dots and (red) solid triangles, and an *N* domain, the lowest line made of (blue) diamonds, in the cell as made. The peak values of absorbance of the *N* and *I* domains are 0.39 and 0.82, respectively. (b) Absorbance of two *I* domains represented with (black) dots and (red) triangles and an *N* domain represented with (blue) squares after a week. The peak values of the *N* and *I* domains are 0.16 and 1.08, respectively. (c) Absorbance of two *I* domains (black dots) and (red diamonds) and *N* domains (red multiplication signs) and (blue squares) after a thermal cycling. The peak values of the *N* and *I* domains are 0.13 and 1.18, respectively. The differences between the peak values of *I* and *N* domains increase as the cell ages and undergoes the thermal cycle. Also shown in the graph (c) is the absorbance of an *M* domain (violet solid triangles) of a mixture (1, 18), which shows negligible absorbance of blue and green light. The order of the legends in the graphs corresponds to the order of the spectra from top to bottom.

200%, respectively. In this experiment, a significant amount of water was lost during the sample preparation and measurement procedure.

C. X-ray diffraction study of the mixture

X-ray diffraction (XRD) results for the mixtures help us to understand the structures and dynamics of the chromonic aggregates. First, the stacking distances of the aggregates of pure SSY and DSCG are 3.42 and 3.35 Å, respectively, as

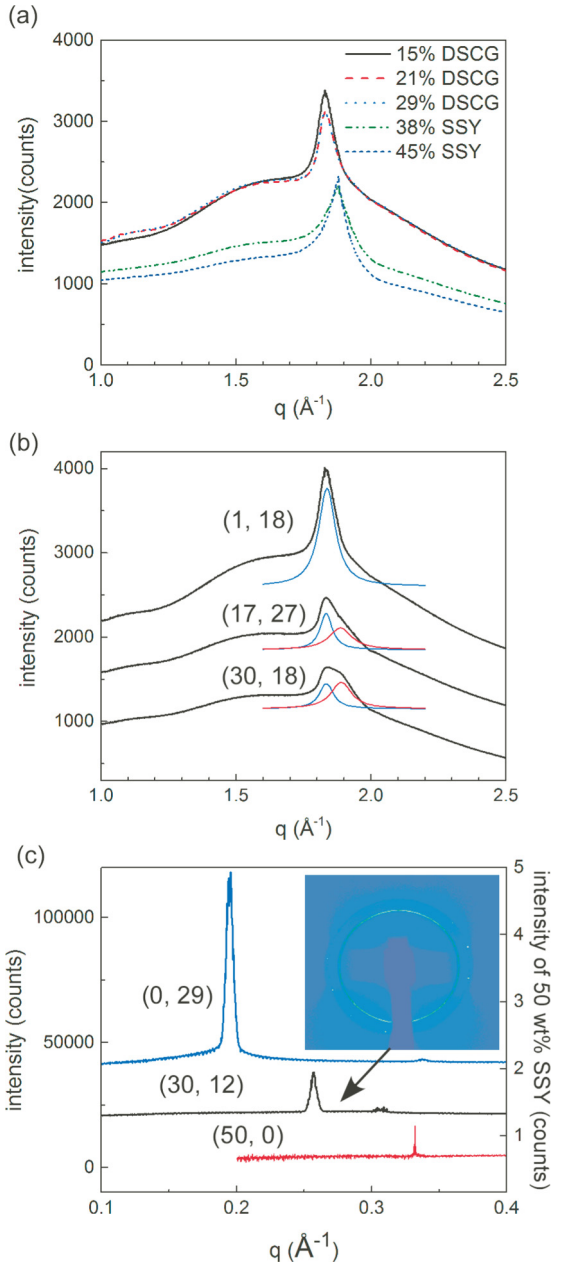

FIG. 8. Large-angle XRD data of pure SSY and DSCG solutions (a) and mixtures (b) in capillaries. Notice in (b) that the peaks are asymmetric and can be fitted to two peaks corresponding to stacking distances of SSY (right peaks) and DSCG (left peaks), as shown in Table I. (c) Small-angle XRD data of an *M* phase DSCG (0, 29) solution, a mixture (30, 12), and an *M* phase SSY (50, 0) solution. The inset shows a diffraction ring corresponding to the main peak at $q = 0.258$ Å^{-1} and diffraction spots corresponding to a collection of small peaks around $q = 0.306$ Å^{-1}, which possibly come from small SSY *M* domains trapped in DSCG *M* domains (see Table II for calculated column distances). The data are shifted from each other along the *y* axes of the graphs to improve visibility.

TABLE I. Chromonic stacking distances of pure SSY, DSCG, and their mixtures. N/A indicates "not available."

Sample (SSY, DSCG)	Chromonic stacking distance (Å)	Coherence length (Å)
(29, 0)	3.33	5.8
(38, 0)	3.35	10.2
(45, 0)	3.35	10.6
(0, 15)	3.43	13.4
(0, 21)	3.42	16.8
(0, 29)	3.42	17.3
(1, 18)	(N/A, 3.42)	(N/A, 13.2)
(17, 27)	(3.33, 3.43)	(9.6, 18.3)
(30, 18)	(3.32, 3.42)	(10.7, 15.8)

shown in Fig. 8(a) and Table I. The stacking distance of pure DSCG matches well with the value reported by other researchers [12]. Looking into this more carefully, we find that the spacing peaks of the mixtures appear clearly asymmetrical and can be fitted to a linear combination of distinct Lorentzian curves whose sizes are proportional to the discrete preparatory concentrations of SSY and DSCG in the mixtures [see Fig. 8(b) and Table I]. This suggests that the stacks are not some mixed ones with intermingled SSY and DSCG stack elements but separate ones of each material.

Second, notice that the mixture (30, 12) has two scattering peaks corresponding to two columnar distances, one corresponding to a small d and the other to a large d, indicating that M domains made of SSY and M domains made of DSCG coexist, as shown in Fig. 6(c). This suggests that the SSY and DSCG columns do not mix in the M phases.

Third, it seems that the SSY-dominant I or N phase compresses the DSCG columns in the M phase so that the lateral distance between the planes of the columns, d, becomes noticeably smaller than that without SSY. For example, $d = 24.4$ Å for a mixture (30, 12) with total concentration of 42 wt % which is 24% smaller than $d = 32.2$ Å for a pure DSCG solution (0, 29) (see Table II). Considering that the concentration of the pure DSCG solution is 0.69% of the total concentration of the mixture, d of the mixture would be $32.2 \times \sqrt{0.69}$ Å $= 26.7$ Å without the compression effect of SSY-rich surrounding phases. This effect is similar to the crowding of SSY aggregates due to a coexisting polyethylene glycol I phase reported by Park and co-workers [15].

IV. DISCUSSION

Sketches of the structure of aggregates and arrangement of aggregates in I, N, $N + I$, and $M + I$ phases of mixtures are shown in Fig. 9. The aggregates in the mixtures are separated into SSY aggregates and DSCG aggregates [see Fig. 9(a)], considering the absence of dichroism of SSY in the DSCG M phase and the distinct stacking distances of the aggregates

TABLE II. Columnar distances of pure solutions and a mixture.

Sample (SSY, DSCG)	Total concentration (wt %)	Distances between planes of columns, d (Å)	Coherence length (Å)
(0, 29)	29	32.2	177
(30, 12)	42	(20.5, 24.4)	(204, 143)
(50, 0)	50	18.9	562

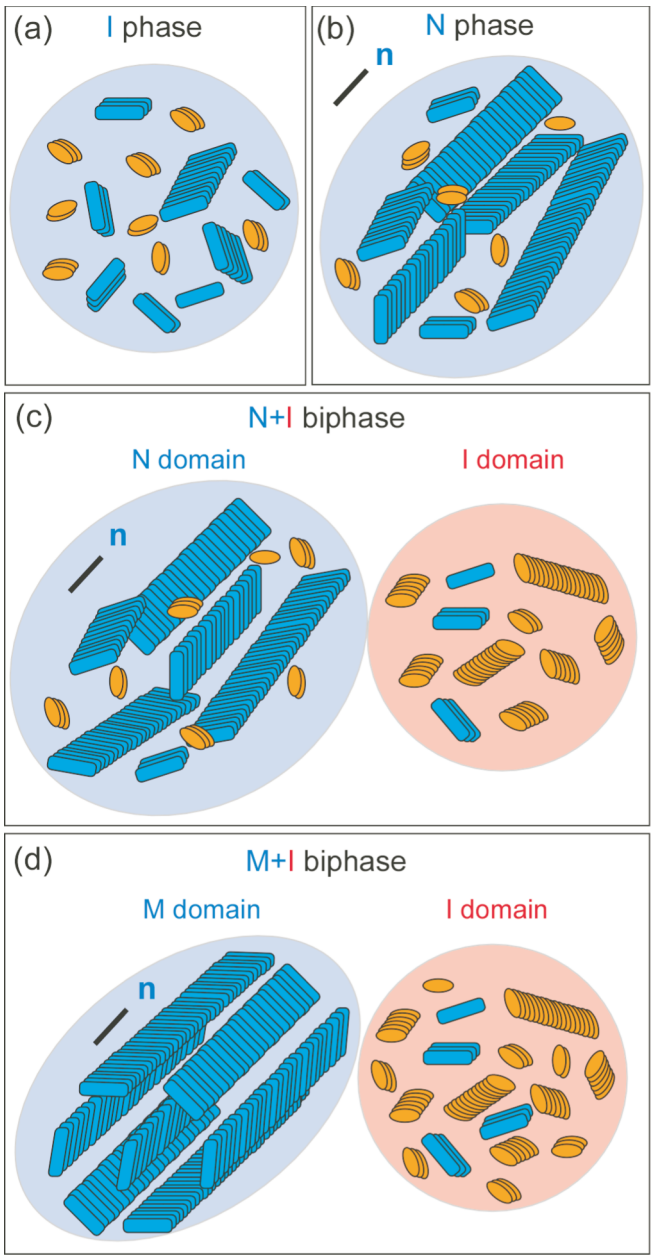

FIG. 9. Structures of mesophases of SSY and DSCG mixtures. DSCG molecules are represented with cyan colored objects and SSY molecules with orange colored objects. (a) When concentrations of both materials are low, the mixture is in the I phase, in which the short aggregates made of each material are well mixed. (b) As DSCG concentration increases, the mixture forms the N phase, in which DSCG aggregates become longer and align with each other to have a preferred direction **n**, while very short SSY aggregates reside in the N domain in random orientations. (c) As SSY is added to the mixture represented in (b), the mixture forms biphasic $N + I$ because the N domain has limitations in containing SSY aggregates in this amount and size. (d) As DSCG concentration of the mixture further increases, the DSCG aggregates grow even longer to form a columnar structure by expelling even the short SSY aggregates over time.

as discussed in the previous section. Stacking of SSY and DSCG molecules together will be energetically unfavorable because of the slightly bent cross section of the core of the DSCG molecule and the different core sizes between the two molecules. Furthermore, phase separation between SSY-rich and DSCG-rich mesophases generally occurs. Coexistence of their aggregates in a domain is allowed only when one material is sparse in the *N* phase [see Fig. 9(b)]. The XRD results and microscopic optical texture of DSCG-rich uniform N phase of a mixture (1, 18) is similar to those of pure nematic DSCG, (0, 18). It is likely that minority aggregates coexist in the majority ones in N phases as far as their sizes are small enough. As the concentration increases above a certain concentration, the size of aggregates of the minority material becomes larger and they are likely to be expelled from the *N* domains to *I* domains [see Fig. 9(c)]. In *M* domains, even very small minority aggregates are expelled to lower phase domains [see Fig. 9(d)].

V. CONCLUSIONS

Mixtures of the two well-known lyotropic chromonic liquid crystal materials sunset yellow FCF (SSY) and disodium Cromoglycate (DSCG) in water show diverse mono-, bi-, and triphasic textures. We observe a tendency for lower-order phase domains to have higher concentration of SSY than the domains with higher-order phases in biphasic or triphasic mixtures. Initial mixing in the isotropic phase results in various degrees of phase separation depending on the concentration, age, and thermal history of the mixtures. These phase behaviors of the mixture are due to both separation of the molecules in the formation of the aggregates and separation of aggregates of the same species by their slow diffusion.

ACKNOWLEDGMENTS

We thank Joseph Maclennan and Matthew Glaser for helpful discussions and comments. This work was supported by U.S. National Science Foundation under Contract No. DMR-1207606 and DMR-1420736. Beamline 7.3.3 of the Advanced Light Source is supported by the Director of the Office of Science, Office of Basic Energy Sciences, of the U.S. Department of Energy under Contract No. DE-AC02-05CH11231.

[1] J. Lydon, J. Mater. Chem. **20**, 10071 (2010).
[2] M. Nakata, G. Zanchetta, B. D. Chapman, C. D. Jones, J. O. Cross, R. Pindak, T. Bellini, and N. A. Clark, Science **318**, 1276 (2007).
[3] T. Shneider and O. D. Lavrentovich, Langmuir **16**, 5227 (2000).
[4] V. G. Nazarenko, O. P. Boiko1, M. I. Anisimov, A. K. Kadashchuk, Y. A. Nastishin, A. B. Golovin, and O. D. Lavrentovich, Appl. Phys. Lett. **97**, 263305 (2010).
[5] S. V. Shiyanovskii, T. Schneider, I. I. Smalyukh, T. Ishikawa, G. D. Niehaus, K. J. Doane, C. J. Woolverton, and O. D. Lavrentovich, Phys. Rev. E **71**, 020702(R) (2005).
[6] F. Guo, A. Mukhopadhyay, B. W. Sheldon, and R. H. Hurt, Adv. Mater. **23**, 508 (2010).
[7] J. E. Halls, R. W. Bourne, K. J. Wright, L. I. Partington, M. G. Tamba, Y. Zhou, T. Ramakrishnappa, G. H. Mehl, S. M. Kelly, and J. D. Wadhawan, Electrochem. Commun. **19**, 50 (2012).
[8] D. J. Edwards, J. W. Jones, O. Lozman, A. P. Ormerod, M. Sintyureva, and G. J. T. Tiddy, J. Phys. Chem. B **112**, 14628 (2008).
[9] Y. A. Nastishin, H. Liu, T. Schneider, V. Nazarenko, R. Vasyuta, S. V. Shiyanovskii, and O. D. Lavrentovich, Phys. Rev. E **72**, 041711 (2005).
[10] H-S. Park, S-W. Kang, L. Tortora, Y. Nastishin, D. Finotello, S. Kumar, and O. D. Lavrentovich, J. Phys. Chem. B **112**, 16307 (2008).
[11] F. Chami and M. R. Wilson, J. Am. Chem. Soc. **132**, 7794 (2010).
[12] W. Xiao, C. Hu, D. J. Carter, S. Nochols, M. D. Ward, P. Laiteri, A. L. Rohl, and B. Kahr, Cryst. Growth Des. **14**, 4166 (2014).
[13] D. M. Agra-Kooijman, G. Singh, A. Lorenz, P. J. Collings, Heinz-S. Kitzerow, and S. Kumar, Phys. Rev. E **89**, 062504 (2014).
[14] V. R. Horowitz, L. A. Janowitz, A. L. Modic, P. A. Heiney, and P. J. Collings, Phys. Rev. E **72**, 041710 (2005).
[15] H-S. Park, S-W. Kang, L. Tortora, S. Kumar, and O. D. Lavrentovich, Langmuir **27**, 4164 (2011).